BIOCHEMISTRY

 Volume 45, Number 42 October 24, 2006

Articles

Enantiomeric Free Radicals and Enzymatic Control of Stereochemistry in a Radical Mechanism: The Case of Lysine 2,3-Aminomutases†

E. Behshad, F. J. Ruzicka, S. O. Mansoorabadi, D. Chen, G. H. Reed, and P. A. Frey*

Department of Biochemistry, University of Wisconsin, 1710 University Avenue, Madison, Wisconsin 73726

Received June 30, 2006; Revised Manuscript Received August 16, 2006

ABSTRACT: The product of *yjeK* in *Escherichia coli* is a homologue of lysine 2,3-aminomutase (LAM) from *Clostridium subterminale* SB4, and both enzymes catalyze the isomerization of (*S*)- but not (*R*)-α-lysine by radical mechanisms. The turnover number for LAM from *E. coli* is 5.0 min^{-1}, 0.1% of the value for clostridial LAM. The reaction of *E. coli* LAM with (*S*)-α-[3,3,4,4,5,5,6,6-$^2H_8$]lysine proceeds with a kinetic isotope effect (k_H/k_D) of 1.4, suggesting that hydrogen transfer is not rate-limiting. The product of the *E. coli* enzyme is (*R*)-*β*-lysine, the enantiomer of the clostridial product. *β*-Lysine-related radicals are observed in the reactions of both enzymes by electron paramagnetic resonance (EPR). The radical in the reaction of clostridial LAM has the (*S*)-configuration, whereas that in the reaction of *E. coli* LAM has the (*R*)-configuration. Moreover, the conformations of the *β*-lysine-related radicals at the active sites of *E. coli* and clostridial LAM are different. The nuclear hyperfine splitting between the C3 hydrogen and the unpaired electron at C2 shows the dihedral angle to be 6°, unlike the value of 77° reported for the analogous radical bound to the clostridial enzyme. Reaction of (*S*)-4-thialysine produces a substrate-related radical in the steady state of *E. coli* LAM, as in the action of the clostridial enzyme. While (*S*)-*β*-lysine is not a substrate for *E. coli* LAM, it undergoes hydrogen abstraction to form an (*S*)-*β*-lysine-related radical with the same stereochemistry of hydrogen transfer from C2 of (*S*)-*β*-lysine to the 5′-deoxyadenosyl radical as in the action of the clostridial enzyme. The resulting *β*-lysyl radical has a conformation different from that at the active site of clostridial LAM. All evidence indicates that the opposite stereochemistry displayed by *E. coli* LAM is determined by the conformation of the lysine side chain in the active site. Stereochemical models for the actions of LAM from *C. subterminale* and *E. coli* are presented.

Lysine 2,3-aminomutase (LAM)[1] from *Clostridium subterminale* SB4 is encoded by the gene *kamA* and catalyzes the interconversion of (*S*)-α-lysine and (*S*)-*β*-lysine (*1*−*3*). This enzyme plays a role in lysine metabolism in species

† Supported by Grant DK28607 from the National Institute of Diabetes and Digestive and Kidney Diseases (P.A.F.), Grant GM35752 from the National Institute of General Medical Sciences (G.H.R.), and by NIH Predoctoral Training Grant T32 GM08293 (S.M.).

* To whom correspondence should be addressed: Department of Biochemistry, University of Wisconsin, 1710 University Ave., Madison, WI 53726. Telephone: (608) 262-0055. Fax: (608) 265-2904. E-mail: frey@biochem.wisc.edu.

[1] Abbreviations: SAM, *S*-adenosyl-(*S*)-methionine; [5′-^{13}C]SAM, (*S*)-[5′-^{13}C]adenosyl-(*S*)-methionine; [5′-$^2H_2$]SAM, (*S*)-[5′-$^2H_2$]adenosyl-L-methionine; PLP, pyridoxal 5′-phosphate; DTT, dithiothreitol; PITC, phenyl isothiocyanate; LAM, lysine 2,3-aminomutase; IPTG, isopropyl *β*-D-thiogalactoside; EPPS, 4-(2-hydroxyethyl)-1-piperazinepropanesulfonic acid; EPR, electron paramagnetic resonance; HPLC, high-performance liquid chromatography; EPR, electron paramagnetic resonance; CD, circular dichroism.

10.1021/bi061328t CCC: $33.50
Published on Web 09/29/2006

Scheme 1

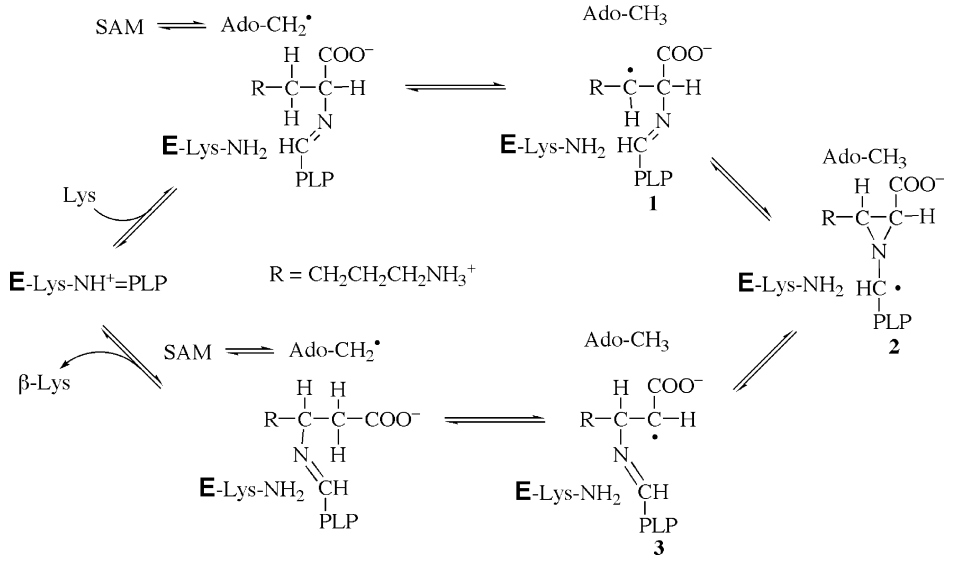

such as *C. subterminale* and *Porphyromonas gingivalis*, whereas in species such as *Streptomyces* sp., β-lysine produced by LAM is a constituent of a family of structurally diverse antibiotics (*4*−*14*). The action of LAM requires SAM, a [4Fe-4S] cluster, and PLP to catalyze the isomerization of (*S*)-α-lysine (*15*−*17*). LAM is a member of the "radical SAM" superfamily, a highly diverse family of enzymes, known members of which use SAM as a radical initiator in catalysis (*18*). This role of SAM is qualitatively unlike its traditional function as the principal biological methylating agent.

Scheme 1 illustrates the chemical mechanism by which clostridial LAM catalyzes the conversion of (*S*)-α-lysine to (*S*)-β-lysine (*15*−*17*, *19*, *20*). This mechanism was established by EPR spectroscopic analysis of the radical intermediates in characterizing their structures and kinetic competencies (*21*−*24*). Reactions of lysine deuterated at C3 proceed with substantial primary deuterium kinetic isotope effects, showing that hydrogen transfer is rate-limiting in the mechanism (*24*). Inasmuch as radical **3** in Scheme 1 accumulates in the steady state, the rate-limiting step is most likely the transfer of hydrogen from the methyl group of 5′-deoxyadenosine to C2 of radical **3**, the product-related radical intermediate.

Currently, there are 53 prokaryotic proteins with amino acid sequences homologous to that of LAM from *C. subterminale* SB4. The aligned amino acid sequences of the *Escherichia coli* protein encoded by the gene *yje*K and of clostridial LAM are 33% identical, and the *E. coli* protein is one of the least similar to clostridial LAM. The active site residues, including those in the CxxxCxxC motif characteristic of radical SAM enzymes, are almost identical between the two enzymes. The residues in hydrogen bonded contact with (*S*)-α-lysine in clostridial LAM include Arg134, Asp293, and Asp330 (*25*). The identities between the enzymes from *C. subterminale* and *E. coli* include Arg134 and Asp293 of the clostridial LAM, but Asp330 is replaced with glutamate (Glu327) in the *E. coli* enzyme (*1*).

The significance of β-lysine in *E. coli* is not known. Unlike *kamA* in *C. subterminale* and *P. gingivalis*, the gene *yjeK* does not appear in a gene cluster associated with lysine metabolism. In *E. coli*, *yjeK* is flanked by genes annotated as elongation factor protein, GroEL/ES chaperone proteins, membrane proteins, and others that seem to be expressed under stress or in the stationary phase. Here we report that the product of *yjeK* is a LAM with low activity relative to that of clostrial LAM, and we show that it functions by an analogous but stereochemically variant mechanism.

EXPERIMENTAL PROCEDURES

Materials. E. coli BL21 Rosetta cells were purchased from Novagen. PLP, ampicillin, chloramphenicol, cysteine, CM-cellulose, (*S*)-4-thialysine, ferric chloride dithionite, ferrous ammonium sulfate, and pyridoxal hydrochloride were purchased from Sigma. SAM was obtained from Sigma as the *p*-toluenesulfonate salt and purified over CM-celluose (*26*). Terrific LB medium and (*S*)-α-lysine hydrochloride were purchased from Fisher Scientific. (*S*)-[3,3-$^2H_2$]-4-Thialysine was prepared as described previously (*22*, *23*). (*S*)-[3,3,4,4,5,5,6,6-$^2H_8$]Lysine, (*S*)-[2-^{2}H]lysine, (*S*)-[2-^{13}C]lysine, and (*RS*)-[α-^{15}N,$^2H_8$]lysine were purchased from CDN Isotopes. IPTG and DTT were purchased from Inalco. Phenyl Sepharose was purchased from Amersham Bioscience.

Overexpression and Purification of E.coli LAM. Expression of *E. coli* LAM was achieved in BL21 Rosetta cells. The cloning of the gene in pET23a has been described previously (*27*). Cells were grown at 37 °C in Terrific LB medium containing 10 μM pyridoxal hydrochloride, 50 μM $FeCl_3$, 100 μg/mL ampicillin, and chloramphenicol (30 μg/mL) to an OD_{600} of 0.9, induced by addition of 1 mM IPTG, and grown for an additional 3 h at 37 °C. The cells were harvested by centrifugation, frozen in liquid nitrogen, and stored at −70 °C.

All purification steps were carried out in a Coy anaerobic chamber. The recombinant protein was purified by the published procedure (*27*) except that the Phenyl Sepharose column was eluted with a stepwise rather than a linear gradient. LAM from *C. subterminale* and LAM from *Bacillus subtilis* were expressed in *E. coli* and purified as described previously (*1*, *27*).

Chemical Characterization of E. coli LAM. The extinction coefficient at 280 nm was measured by quantitative analysis

of PITC-amino acids (28) after complete acid hydrolysis of solutions of the enzyme obtained after reconstitution of the iron−sulfur clusters and measurement of A_{280}. The procedure has been described for clostridial LAM (29). The iron, inorganic sulfide, and PLP contents of *E. coli* LAM were measured by published procedures (*30*−*32*).

Reconstitution of [4Fe−4S] Clusters. Reconstitution of iron−sulfur clusters was based on a published method (*33*). To LAM at 10 mg/mL under anaerobic conditions were added DTT, sodium sulfide, and ferrous ammonium sulfate to final concentrations of 5, 1.2, and 1.2 mM, respectively, and the mixture was incubated at ambient temperature for 3 h. The reconstituted protein was separated from iron and sulfide complexes by gel permeation chromatography over a column of Sephacryl S-200 equilibrated in 0.1 M EPPS (pH 8).

Reductive Activation and Assay. LAM was mixed with the reductive incubation buffer [200 mM EPPS (pH 8.0), 36 mM ferrous ammonium sulfate, 24 mM PLP, and 10 mM (*S*)-cysteine] under anaerobic conditions in a ratio of 3:1 (v/v) and incubated for 3 h at 37 °C. The assay of activated LAM was the procedure of Miller et al., in which the PITC derivative of (*S*)-*β*-lysine that was produced was separated from that of (*S*)-α-lysine by HPLC and measured spectrophotometrically (*23*).

Synthesis of (S)-β-[2-^{13}C]Lysine and (2S,3R)-β-[2-$^{2}H_1$]-Lysine. (*S*)-α-[2-^{13}C]Lysine (250 mM) was incubated with 30 μM LAM from *C. subterminale*, 150 μM SAM, 1 mM sodium dithionite, and 200 mM EPPS (pH 8.0) for 24 h at room temperature in the anaerobic chamber. Analysis by HPLC indicated 87% conversion of (*S*)-α-[2-^{13}C]lysine to (*S*)-*β*-[2-^{13}C]lysine at equilibrium. (*S*)-*β*-[2-^{13}C]Lysine was separated from (*S*)-α-[2-^{13}C]lysine by chiral chromatography using a Chirobiotic T column (Astec) equilibrated in 50 mM sodium phosphate buffer (pH 3.1). The retention times for (*S*)-α- and (*S*)-*β*-[2-^{13}C]lysine were 5.7 and 6.8 min, respectively, under the conditions that were employed. (*S*)-*β*-[2S-^{2}H]Lysine from (*RS*)-α-[2-^{2}H]lysine was prepared by the same procedure. The retention time for (*R*)-α-[2-^{2}H]lysine in this experiment was found to be 7.3 min.

Synthesis of [5′-^{13}C]SAM and [5′-$^{2}H_2$]SAM. SAM with ^{13}C at C5′ or deuterium bonded to C5′ was synthesized from the correspondingly labeled ATP and methionine by use of SAM synthetase as described elsewhere (*34*).

Synthesis and Ultraviolet CD of PITC-(R)-β-Lysine. LAM from *E. coli* (0.5 mM) was used to produce *β*-lysine by the procedure described above in 30 mM EPPS buffer (pH 8.0), 20 mM (*S*)-α-lysine, 5 mM sodium dithionite, and 3 mM SAM. The purified *β*-lysine was derivatized with PITC and purified by HPLC over a C18 column. A sample of PITC-(*S*)-*β*-lysine was produced in parallel using the LAM from *C. subterminale*. CD spectra of the purified PITC-*β*-lysines were recorded against water as a reference at 1 nm resolution between 215 and 350 nm in a quartz cell with a path length of 1 mm at 25 °C with an Aviv 62 DS CD spectrometer in the Biophysical Instrumentation Facility of the Department of Biochemistry.

EPR Spectroscopy. Samples of LAM from *E. coli* at concentrations of 200−250 μM and with iron−sulfur clusters reconstituted were prepared in EPR tubes in the glovebox. The samples were prepared in 200 mM EPPS (pH 8), 5 mM sodium dithionite, and 1.13 mM SAM. The reactions were initiated by addition of isotopically labeled or unlabeled (*S*)-α-lysine, (*S*)-*β*-lysine, or (*S*)-4-thialysine. The EPR sample tubes were frozen within 20−40 s in isopentane cooled in a liquid nitrogen bath. After being frozen, the EPR samples were removed from the anaerobic chamber and stored in liquid N_2. For EPR analysis at 77 K at X-band on a Varian E3 spectrophotometer, the instrument settings were as follows: microwave frequency, 9.1 GHz; modulation amplitude, 1.6 G; and microwave power, 5.00 mW (unless noted otherwise). A standard liquid nitrogen immersion dewar was used. The spectrometer was interfaced with a computer for data acquisition and analysis. Simulations of spectra were performed as described previously (*21*).

RESULTS

Characterization of LAM from E. coli. On the basis of quantitative amino acid and spectrophotometric analyses, the extinction coefficient of *E. coli* LAM at 280 nm is 4.6×10^5 M^{-1} cm^{-1}. The enzyme with reconstituted iron−sulfur clusters contains 3.7 mol of iron and 3.8 mol of sulfide per mole of subunits. The values of steady-state kinetic parameters are as follows: $k_{cat} = 4.8$ min^{-1}, $K_m = 5$ mM, and $k_{cat}/K_m = 1$ mM^{-1} min^{-1} at pH 8.0 and 25 °C. In terms of k_{cat} values, LAM from *E. coli* is 0.1% as active as clostridial LAM, but it displays a similar value of K_m. Like the clostridial enzyme, LAM from *E. coli* will not accept (*S*)-ornithine or (*R*)-α-lysine as a substrate. Unlike the clostridial enzyme, which displays a substantial deuterium kinetic isotope effect in the reaction of (*S*)-[3,3,4,4,5,5,6,6-$^{2}H_8$]lysine, LAM from *E. coli* displays a small effect (k_H/k_D) of 1.4 at either 40 or 90 mM substrate. Also unlike the clostridial enzyme, LAM from *E. coli* undergoes suicide inactivation in a substrate-dependent process over a period of 15−20 min. The chemical nature of the inactivation is not known; however, it is not accompanied by the destruction of SAM.

(*R*)-*β-Lysine as the Product*. Certain properties of *E. coli* LAM detailed below, in particular, the EPR spectra observed in its reactions with (*S*)-lysine and (*S*)-*β*-lysine, the product of clostridial LAM, suggested a structural difference in the products of the two enzymes. Inasmuch as the retention times for the PITC derivatives of the products upon reversed phase HPLC were identical, it was possible that the two might be enantiomeric, that is, that the *E. coli* product could be (*R*)-*β*-lysine. Because of the low activity of the *E. coli* enzyme and its suicide inactivation, it proved to be difficult to generate large amounts of the product for polarimetric analysis. In a more sensitive test, the Cotton effects associated with the chromophore in PITC-*β*-lysines allowed the configurations of the *E. coli* and clostridial products to be compared by CD spectrophotometry. The resulting curves in Figure 1 show that the two PITC derivatives display opposite Cotton effects, positive for PITC-(*S*)-*β*-lysine from *C. subterminale* LAM and negative for the PITC-*β*-lysine from *E. coli*. Therefore, inasmuch as the clostridial enzyme produces (*S*)-*β*-lysine (*3*), the *E. coli* enzyme must produce (*R*)-*β*-lysine.

Stereochemical analysis of the product of LAM from *B. subtilis* by the procedure described above led to the same Cotton effect that was seen for *β*-lysine from clostridial LAM, showing that the *B. subtilis* product is (*S*)-*β*-lysine.

Characterization of a Lysyl-Free Radical Intermediate. A substrate-based radical bound to *E. coli* LAM is observed

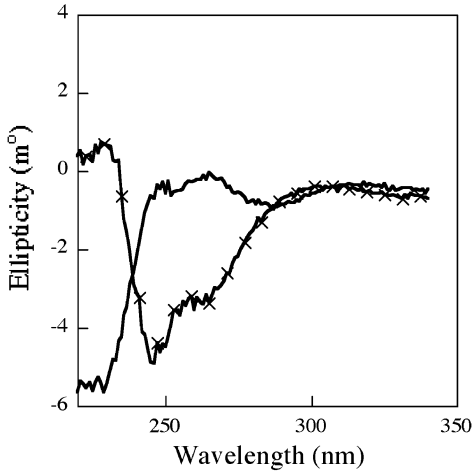

FIGURE 1: UV circular dichroism spectra for PITC derivatives of (*S*)-*β*-lysine (—) and (*R*)-*β*-lysine produced in the reaction of *E. coli* LAM (—×—).

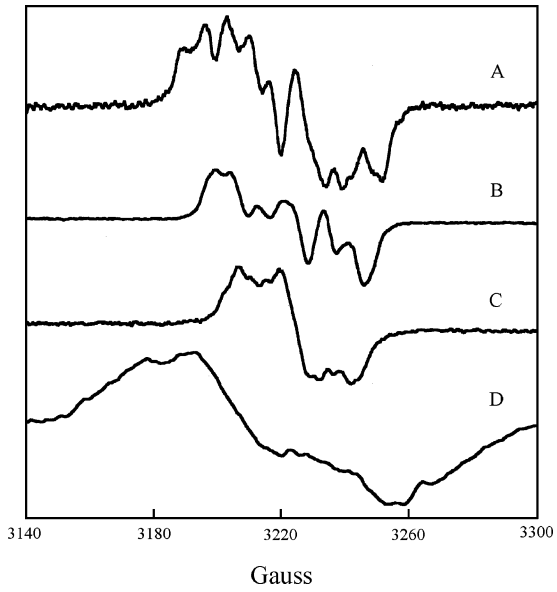

FIGURE 2: EPR spectra of the radical from (*S*)-α-lysine at the active site of *E. coli* LAM. The EPR samples were prepared under anaerobic conditions with 200 *μ*M *E. coli* LAM, 1.1 mM SAM, 2.5 mM dithionite, and 200 mM EPPS buffer (pH 8.0). The EPR spectra were recorded at 77 K: (A) 40 mM α-(*S*)-lysine, (B) 40 mM (*S*)-α-[3,3,4,4,5,5,6,6-$^{2}H_{8}$]lysine, (C) 40 mM (*S*)-α-[2-^{2}H]-lysine, and (D) 40 mM [2-^{13}C]lysine. The spectra show that the dominant radical in the steady state is the *β*-lysyl radical, **3** in Scheme 1.

by EPR at 77 K after freeze-quenching in the steady state (Figure 2A). The EPR spectra of samples prepared with (*S*)-α-[3,3,4,4,5,5,6,6-$^{2}H_{8}$]lysine show weak nuclear hyperfine splitting of at least one hydrogen from C3 to C6 of the lysyl side chain with the unpaired electron. The overall splitting pattern is similar to that of the unlabeled compound, while individual features are slightly narrowed (compare panels A and B of Figure 2). The principal location of the unpaired electron is C2 of the lysyl carbon skeleton, as shown by the spectra in panels C and D of Figure 2. The complex nuclear hyperfine splitting pattern is narrowed and simplified with the substitution of ^{2}H for ^{1}H at C2. Comparison of panel C with panel A or B shows that the unpaired electron is engaged in strong nuclear hyperfine coupling with C2(H), and its replacement with deuterium leads to a narrowed

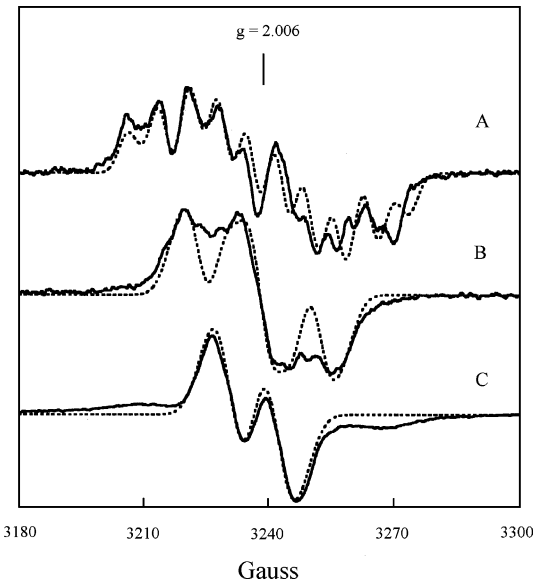

FIGURE 3: Simulated EPR spectra of *β*-lysyl radicals at the active site of *E. coli* LAM. Experimental and simulated spectra of the *β*-lysyl radical are shown for the species generated with (*S*)-α-[2-^{2}H]lysine, (*RS*)-α-[2-^{15}N,2,3,3,4,4,5,5,6,6-$^{2}H_{9}$]lysine, and unlabeled (*S*)-α-lysine in the active site of *E. coli* LAM. (A) Spectrum (—) and simulation (- - -) of the radical generated upon addition of 40 mM (*S*)-α-lysine to 180 *μ*M enzyme. (B) Spectrum (—) and simulation (- - -) of the radical generated upon addition of 40 mM (*S*)-α-[2-^{2}H]lysine. The samples were frozen within 30−40 s of addition of substrate. (C) Spectrum (—) and simulation (- - -) of the radical generated upon addition of 80 mM (*RS*)-α-[2-^{15}N,2,3,3,4,4,5,5,6,6-$^{2}H_{9}$]lysine. Parameters used for the calculation of simulated spectra are given in Table 1.

signal. The nuclear hyperfine splitting for deuterium is much smaller (approximately one-sixth) than that for hydrogen (*35*). Further, samples prepared with (*S*)-[2-^{13}C]lysine exhibit strong broadening of the EPR signals (Figure 2D), because of the large nuclear hyperfine splitting tensor of ^{13}C at the center of an unpaired spin (*35*). The results showing spin localized at C2 of lysine are consistent with the product-related free radical **3** in Scheme 1 being the principal radical intermediate in the steady state.

The spectral envelope of the product-related radical (Figure 2) is very different from that reported for the analogous radical at the active sites of clostridial and *Bacillus* LAM (*21*, *27*). Differences in the spectra arise from differences in the conformations about the C2−C3 bond. The variant dihedral angles of the *β*-C3 substituents bring about different nuclear hyperfine splitting from the *β*-hydrogen and *β*-nitrogen. Simulations of the spectra for samples prepared with (*RS*)-[2-^{15}N,2,3,3,4,4,5,5,6,6-$^{2}H_{9}$]lysine, (*S*)-[2-^{2}H]lysine, and unlabeled (*S*)-lysine allowed the splitting constants to be evaluated by the procedures employed to characterize the corresponding radical in clostridial LAM (*21*). The spectra and simulations are shown in Figure 3, and the splitting constants from the simulations are assembled in Table 1. The isotropic hyperfine splittings arising from *β*-substituents in *π*-radicals are strongly dependent on the dihedral angles (*χ*) defined in Scheme 2. For *β*-proton splittings, $a_{\beta H}$, the following relationship has been established: $a_{\beta H} = A_1 + A_2 \cos^2 \chi$ (*36*). Values of A_1 and A_2 are empirically determined constants that have values of 0.92 and 42.6 G, respectively, for unit spin density on Cα. The dihedral angles relating the spin-bearing p-orbital to the positions of H_β and N_β in *E.*

Table 1: Hyperfine Splitting Parameters Obtained from Spectral Simulations

		principal values of the hyperfine tensor (G)		
nucleus	a_o (G)	A_{xx}	A_{yy}	A_{zz}
$^1H_\alpha$	19.5	38.5	0	20
$^2H_\alpha$	3.0	5.9	0	3.1
$^1H_\beta$	13.5		isotropic	
$^2H_\beta$	2.1		isotropic	
$^{14}N_\beta$	7.8		isotropic	
$^{15}N_\beta$	11		isotropic	

coli LAM (shown at the right in Scheme 2) are 6° and 50°, respectively. In contrast, the corresponding angles in the enantiomeric radical bound to clostridial LAM (shown at the left in Scheme 2) are 77° (H_β) and 17° (N_β), respectively.

The spectrum shown in Figure 3C contains flanking shoulders that are not included in the simulations. These shoulders are attributed to the presence of radicals elicited by contaminating unlabeled lysine: the commercial compound is only 90% deuterated.

(S)-4-Thialysine and Radical ***1.*** (*S*)-4-Thialysine is an alternative substrate for *C. subterminale* LAM (*22*, *23*). The ultimate products from (*S*)-4-thialysine are *β*-mercaptoethylamine and formyl acetate, because of the chemical instability of *β*-4-thialysine. Figure 4 shows the EPR signal generated when (*S*)-4-thialysine or (*RS*)-4-thia[3,3-$^2H_2$]lysine is added to reductively activated *E. coli* LAM together with dithionite and SAM and then frozen in liquid N_2 within 3 min. The hyperfine splitting in the labeled sample is narrower than in the unlabeled one, suggesting that the unpaired electron resides on C3. Thus, as in the case of clostridial LAM, the 4-thia analogue of radical **1** in Scheme 1 accumulates in the steady state of the reaction of (*S*)-4-thialysine.

Radical Formation with (S)-β-Lysine. (*S*)-*β*-Lysine is the product of clostridial and *Bacillus* LAM, whereas (*R*)-*β*-lysine is the product of *E. coli* LAM. Nonetheless, addition of (*S*)-*β*-lysine to activated *E. coli* LAM leads to radical formation, as shown by the EPR spectra in Figure 5. Figure 5A shows the resultant EPR spectrum upon addition of (*S*)-*β*-lysine to *E. coli* LAM. The splitting pattern of this radical is very different from that observed upon addition of (*S*)-α-lysine (Figures 2 and 3). Within 30 min, the radical signal weakens. The radical is an isomer of the one generated from (*S*)-α-lysine as shown by the qualitative order of the hyperfine splittings in the spectrum generated with (*S*)-*β*-[2-^{13}C]lysine (Figure 5B). The large ^{13}C broadening and the additional features constitute direct evidence that the unpaired electron resides on C2 of the carbon skeleton. The results strongly imply that the 5′-deoxyadenosyl radical derived from SAM abstracts a hydrogen atom from C2 of (*S*)-*β*-lysine. The resulting lysyl radical and that generated from (*S*)-α-lysine in Figures 2 and 3 must be isomers of radical **3** in Scheme 1. Radical **3** has a single optical center, that at C3, which has the (*R*)-configuration at the active site of *E. coli* LAM when it is generated from (*S*)-α-lysine (Figure 1). The enantiomeric (*S*)-isomer of radical **3** must be produced in the reaction of (*S*)-*β*-lysine. There is currently no evidence that the reaction of (*S*)-*β*-lysine proceeds further in the reverse direction.

FIGURE 4: EPR spectra of the radical induced at the active site of *E. coli* LAM by (*S*)-4-thialysine. The solid line was generated upon addition of 80 mM (*RS*)-4-thialysine, and the dashed line is for the radical formed upon addition of 80 mM (*RS*)-4-thia[3,3-$^2H_2$]-lysine. The samples contain 2.5 mM dithionite, 1.5 mM SAM, and 200 mM EPPS (pH 8). Samples were frozen within 1 min of the addition of the substrate. The spectra indicate that the dominant radical in the steady state is the 4-thia analogue of radical **1** in Scheme 1.

When the (*S*)-enantiomer of radical **3** at the active site of clostridial LAM abstracts a hydrogen atom from 5′-deoxyadenosine, the hydrogen atom enters the 2-*pro-R* position of C2 on the pathway to (*S*)-*β*-lysine. The stereochemistry

Scheme 2

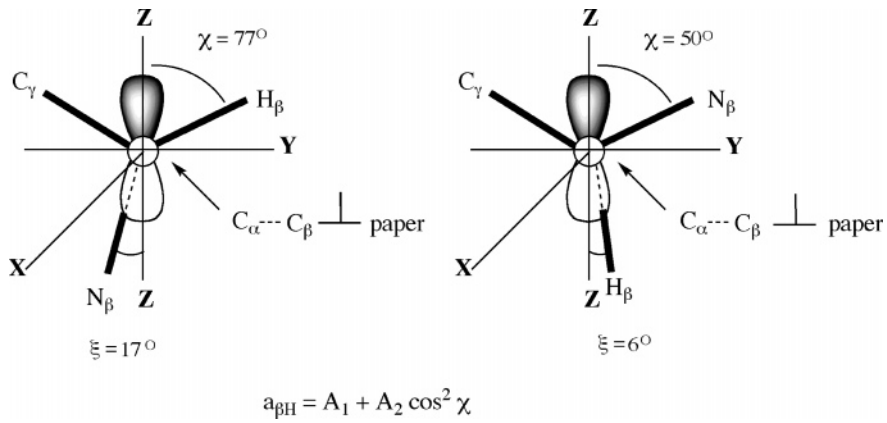

$$a_{\beta H} = A_1 + A_2 \cos^2 \chi$$

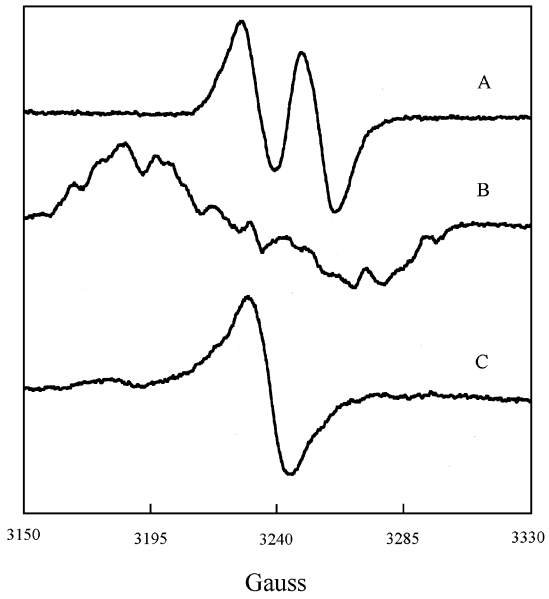

FIGURE 5: EPR spectra of the (*S*)-β-lysyl radical at the active site of *E. coli* LAM. (A) Radical generated upon addition of 70 mM (*S*)-β-lysine. (B) Radical generated upon addition of 27 mM (*S*)-β-[2-^{13}C]lysine. EPR samples were prepared with 200 μM enzyme, 2.5 mM dithionite, and 1.3 mM SAM in 200 mM EPPS (pH 8.0) and were frozen within 20−25 s of the addition of substrate. (C) Radical formed upon addition of 1 mM (*S*)-β-[2-^{2}H]lysine. The samples contained 40 μM enzyme, 2.5 mM dithionite, 0.3 mM SAM, and 200 mM EPPS (pH 8.0) and were frozen within 20 s of the addition of the substrate. The modulation amplitude was set at 8 G.

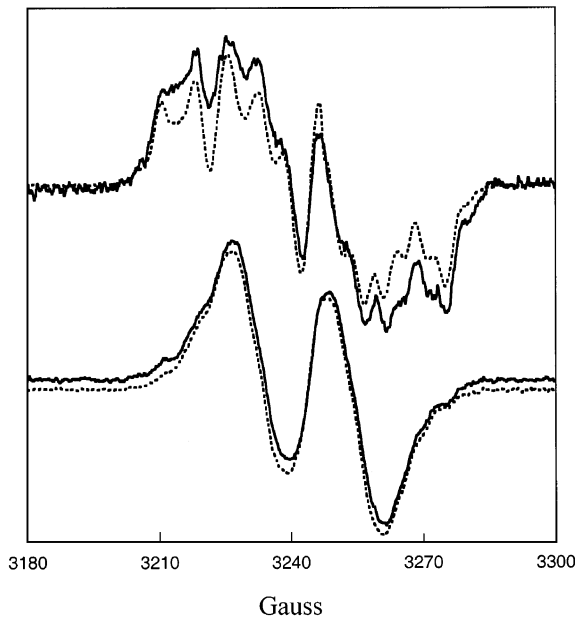

FIGURE 6: Effects of [5′-$^{2}H_2$]SAM on the EPR spectrum of β-lysyl radicals at the active site of *E. coli* LAM. The top spectra are of the (*R*)-β-lysyl radical formed with (*S*)-α-lysine in the presence of SAM (—) or [5′-$^{2}H_2$]SAM (- - -). The bottom spectra are of the (*S*)-β-lysyl radical formed with SAM (—) or [5′-$^{2}H_2$]SAM (- - -).

of hydrogen transfer to the (*R*)-isomer of radical **3** at the active site of *E. coli* LAM can be addressed by preparing (*S*)-β-[2R-^{2}H]lysine and determining whether hydrogen or deuterium is transferred to the 5′-deoxyadenosyl radical when added to *E. coli* LAM to generate the (*S*)-isomer of radical **3**. If deuterium is transferred, the EPR signal will be the doublet in Figure 5A; if hydrogen is transferred, the smaller nuclear hyperfine coupling of the remaining deuterium will lead to a broadened singlet spectrum. As shown in Figure 5C, the signal is a broadened singlet, proving that deuterium is retained at C2 in the radical. Therefore, the stereochemistry of hydrogen transfer at C2 of (*S*)-β-lysine is the same for the *E. coli* and clostridial LAM.

*Effects of [5′-$^{2}H_2$]SAM on EPR Spectra of (R)- and (S)-Radical **3***. The turnover number of *E. coli* LAM is 0.1% of that of LAM from *C. subterminale*. Because hydrogen transfer from 5′-deoxyadenosine to radical **3** in Scheme 1 limits the rate of the action of the clostridial enzyme, and radical **3** accumulates to observable levels in the reactions of both enzymes, it is conceivable that slower turnover by the *E. coli* enzyme could be due to the absence of close contact between C2 in radical **3** and the methyl group of 5′-deoxyadenosine. These atoms are in van der Waals contact in the case of clostridial LAM (*34*).

Comparisons of the EPR spectra in Figure 6 for samples of the (*R*)-isomer of radical **3** bound to *E. coli* LAM prepared with (*S*)-α-lysine and SAM, [5′-$^{2}H_2$]SAM, suggest that the methyl group of 5′-deoxyadenosine is in van der Waals contact with C2 of the lysyl group bearing the unpaired electron in radical **3**. In the top spectra of Figure 6, the solid line is the spectrum with SAM and the dashed line is that with [5′-$^{2}H_2$]SAM. Distinct narrowing of the features with [5′-$^{2}H_2$]SAM indicates that C2 of radical **3** and deuterium of 5′-deoxy[5-$^{2}H_2$]adenosine are in van der Waals contact. The smaller magnetogyric ratio for deuterium relative to hydrogen (*35*) leads to narrowed and sharpened features because of through-space nuclear hyperfine coupling of deuterium with the unpaired electron at C2 in the (*R*)-isomer of radical **3**. The results do not support a hypothesis which holds that the difference in activity between the *E. coli* and clostridial LAM can be attributed to a difference in contact distance between 5′-deoxyadenosine and radical **3** in the mechanism. The bottom spectra in Figure 6 are analogous to the EPR spectra when the (*S*)-isomer of radical **3** is generated with (*S*)-β-lysine and SAM, [5′-$^{2}H_2$]SAM at the active site of *E. coli* LAM. The spectra with ^{2}H or ^{1}H have broader intrinsic line widths and make it more difficult to detect weak hyperfine splitting.

DISCUSSION

Stereochemistry and Mechanism. The central facts in comparing the actions of *E. coli* LAM with the corresponding enzymes from *C. subtermiale* and *B. subtilis* are that all three function by similar reaction mechanisms. β-Lysine-related free radicals are intermediates in the steady states of all three reactions (refs *21* and *26* and this work), and the *E. coli* and clostridial enzymes both produce the substrate-related radical **1** in Scheme 1 with (*S*)-4-thialysine as the substrate (refs *22* and *23* and this work).

Identical and variant stereospecificities characterize the actions of these enzymes. All three accept only the (*S*)-stereoisomer of lysine, and the clostridial and *Bacillus* enzymes produce the (*S*)-stereoisomer of β-lysine; however, the *E. coli* enzyme produces (*R*)-β-lysine. The variant conformations of the steady-state radicals in the reactions of the *E. coli* and clostridial LAMs in Scheme 2 are likely determined by the fact that they are enantiomers constrained to fit within similar active sites. In the structure of clostridial

LAM, lysine is bound by three main interactions: the α-carboxylate makes an ionic contact with Arg134, the α- or *β*-amino group is bound as an imine to PLP, and the *ϵ*-aminium group makes ionic contacts with Asp293 and Asp330. The contact amino acids are conserved in the *E. coli* enzyme, except that Asp330 in clostridial LAM is a glutamate residue in *E. coli* LAM. If the amino acid contacts with the enantiomeric radicals **3** (Scheme 1) in the clostridial enzyme are conserved in the *E. coli* enzyme, the radicals must have different conformations, as they do. The identical stereochemistry of abstraction of hydrogen from (*S*)-*β*-lysine by the clostridial and *E. coli* enzymes also requires an explanation.

The left side of Figure 7 illustrates the stereochemical course of the action of clostridial LAM in producing (*S*)-*β*-lysine. The configuration at C3 of *β*-lysine is determined by the conformation of the lysyl side chain in the substrate-related radical **1** (Scheme 1). The analogous transformation to produce (*R*)-*β*-lysine illustrated in the right side of Figure 7 shows that a variant conformation of the lysyl side chain can lead to the (*R*)-configuration in the azacyclopropylcarbinyl radical **2** and in the product. The variant conformation is more sterically restricted so that the side chain is less extended. The process naturally leads to different conformations in the product-related radicals, as observed and illustrated in Scheme 2. One can speculate that restricted binding of the lysyl side chain in the *E. coli* enzyme might be caused by the steric bulk of a glutamate residue in place of Asp330 in the clostridial active site. The hypothetical conformations in the sequence on the right in Figure 7 suggest that the action of *E. coli* LAM leads to abstraction of the 3-*pro-S* hydrogen from (*S*)-α-lysine, unlike the abstraction of the 3-*pro-R* hydrogen in the reaction of the clostridial enzyme (*3*).

Both reaction sequences in Figure 7 lead to the same stereochemistry of hydrogen transfer to C2 of (*S*)-*β*-lysine by clostridial LAM and C2 of (*R*)-*β*-lysine by *E. coli* LAM. This hypothetical stereochemistry is inspired by the likelihood that the binding of the *β*-amino group to PLP and binding of α-carboxylate to Arg134 control the stereochemistry. The fact that both *E. coli* and clostridial LAM catalyze abstraction of the 2-*pro-R* hydrogen from (*S*)-*β*-lysine supports but does not prove this model.

Activity of E. coli LAM. The low activity of *E. coli* LAM relative to that of the clostridial enzyme raises the question of whether (*S*)-α-lysine is the true substrate for LAM in *E. coli*. Because the functions of variant forms of the same enzyme in different organisms are often different, they frequently display different activities. The classic case is the alcohol dehydrogenases from horse liver and yeast, which differ by 100-fold in catalytic activity yet are structurally and apparently mechanistically similar. A similar difference in activity has been noted for LAM from *C. subterminale* and *B. subtilis* (*27*), and *E. coli* LAM is even less active than the *Bacillus* enzyme.

The low activities of the *Bacillus* and *E. coli* enzymes may be related to their biological functions and the needs of these organisms. Clostridia use LAM in the metabolism of (*S*)-α-lysine as a source of carbon and nitrogen and so require a high activity. In other organisms, *β*-lysine is used in cellular defense mechanisms, such as the production of antibiotics (*4*−*14*). In *E. coli* and *Bacillus* sp., high activity may not be beneficial in the production of the few molecules of *β*-lysine required to produce a specialized molecule. Low activities are not uncommon in enzymes that produce specialized molecules such as antibiotics, examples being the tyrosine 2,3-aminomutase required for the biosynthesis of the antitumor antibiotic C-1027 and the lysine cyclodeaminase

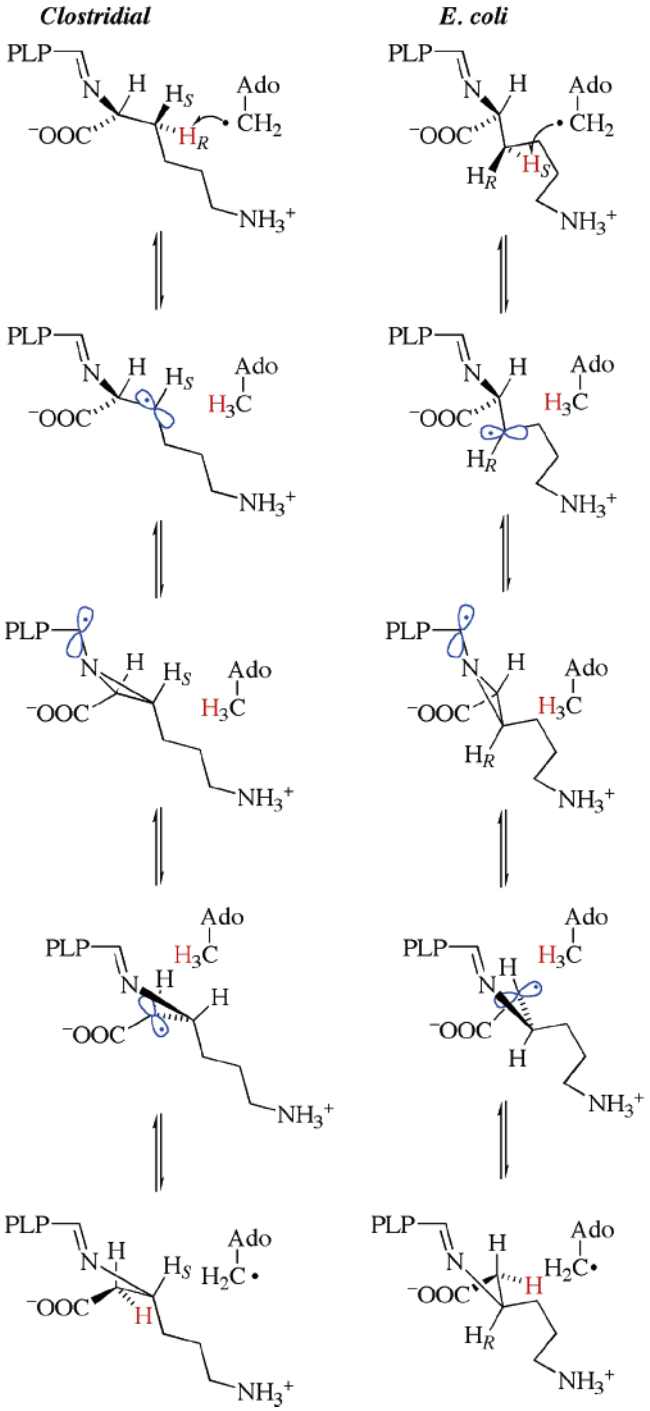

FIGURE 7: Stereochemical models for the mechanisms of reactions of LAM from *C. subterminale* and *E. coli*. The sequence on the left depicts the mechanism and stereochemistry for the reaction of *C. subterminale* LAM, and that on the right depicts the hypothetical mechanism and stereochemistry of the action of *E. coli* LAM. Available evidence indicates that the basic chemistry is the same for the two enzymes but the stereochemistry is different for the initial hydrogen abstraction by the 5′-deoxyadenosyl radical and cyclization to the azacyclopropylcarbinyl radical intermediate. The stereochemistry of the transfer of hydrogen to C2 of *β*-lysine is postulated, but not proven, to be the same for the two enzymes.

required in the biosynthesis of rapamycin (*37*, *38*). The latter enzymes display turnover numbers that are approximately one-eighth of that of LAM from *E. coli*. It seems likely that if (*S*)-α-lysine is the unique substrate for *E. coli* LAM, the function of this enzyme in *E. coli* should be the production of a specialized molecule.

REFERENCES

1. Ruzicka, F. J., Lieder, K. W., and Frey, P. A. (2000) Lysine 2,3-aminomutase from *Clostridium subterminale* SB4: Mass spectral characterization of cyanogen bromide-treated peptides and cloning, sequencing, and expression of the gene *kamA* in *Escherichia coli*, *J. Bacteriol. 182*, 469−476.
2. Chirpich, T. P., Zappia, V., Costilow, R. N., and Barker, H. A. (1970) Lysine 2,3-aminomutase. Purification and properties of a pyridoxal phosphate and S-adenosylmethionine-activated enzyme, *J. Biol. Chem. 245*, 1778−1789.
3. Aberhart, D. J., Gould, S. J., Lin, H.-J., Thiruvengadam, T. K., and Weiller, B. H. (1983) Stereochemistry of Lysine 2,3-Aminomutase Isolated from *Clostridium subterminale* Strain SB4, *J. Am. Chem. Soc. 105*, 5461−5470.
4. Grammel, N., Pankevych, K., Demydchuk, J., Lambrecht, K., Saluz, H. P., and Krugel, H. (2002) A β-lysine adenylating enzyme and a β-lysine binding protein involved in poly β-lysine chain assembly in nourseothricin synthesis in *Streptomyces noursei*, *Eur. J. Biochem. 269*, 347−357.
5. Singh, K., Sehgal, S. N., Rakhit, S., and Vezina, C. (1983) Isolation of a *Streptomyces rochei* idiotroph requiring β-lysine for production of streptothricin, *J. Antibiot. 36*, 1770−1773.
6. Miyaki, T., Tenmyo, O., Numata, K., Matsumoto, K., Yamamoto, H., Nishiyama, Y., Ohbayashi, M., Imanishi, H., Konishi, M., and Kawaguchi, H. (1981) Tallysomycin, a new antitumor antibiotic complex related to bleomycin. IV. New biosynthetic derivatives of tallysomycin, *J. Antibiot. 34*, 658−664.
7. Nomoto, S., Teshima, T., Wakamiya, T., and Shiba, T. (1977) The revised structure of capreomycin, *J. Antibiot. 30*, 955−959.
8. Sawada, Y., and Taniyama, H. (1977) Studies on the β-lysine peptide. IV. Preparation of semi-synthetic racemomycins and their antimicrobial activities, *Chem. Pharm. Bull. 25*, 1302−1305.
9. Carter, J. H., II, Du Bus, R. H., Dyer, J. R., Floyd, J. C., Rice, K. C., and Shaw, P. D. (1974) Biosynthesis of viomycin. II. Origin of β-lysine and viomycidine, *Biochemistry 13*, 1227−1233.
10. Seltmann, G. (1989) Biochemical aspects of the resistance to nourseothricin (streptothricin) of *Escherichia coli* strains, *J. Basic Microbiol. 29*, 547−559.
11. Inamori, Y., Amino, H., Tsuboi, M., Yamaguchi, S., and Tsujibo, H. (1990) Biological activities of racemomycin-B, β-lysine rich streptothricin antibiotic, the main component of *Streptomyces lavendulae* OP-2, *Chem. Pharm. Bull. 38*, 2296−2298.
12. French, J. C., Bartz, Q. R., and Dion, H. W. (1973) Myomycin, a new antibiotic, *J. Antibiot. 26*, 272−283.
13. Gould, S. J., Martinkus, K. J., and Tann, C.-H. (1981) Biosynthesis of Streptothricin F. 1. Observing the interaction of primary and secondary metabolism with [1,2-^{13}C]acetate, *J. Am. Chem. Soc. 103*, 2871−2872.
14. Gould, S. J., and Thiruvengadam, T. K. (1981) Studies of nitrogen metabolism using ^{13}C NMR Spectroscopy. 3. Synthesis of DL-[3-^{13}C,2-^{15}N]lysine and its incorporation into Streptothricin F, *J. Am. Chem. Soc. 103*, 6752−6754.
15. Frey, P. A., and Magnusson, O. Th. (2003) *S*-Adenosylmethionine: A wolf in sheep's clothing, or a rich man's adenosylcobalamin? *Chem. Rev. 103* (6), 2129−2148.
16. Frey, P. A., and Booker, S. J. (2001) Radical mechanisms of S-adenosylmethionine-dependent enzymes, *Adv. Protein Chem. 58*, 1−45.
17. Frey, P. A. (2001) Radical mechanisms of enzymatic catalysis, *Annu. Rev. Biochem. 70*, 121−148.
18. Sofia, H. J., Chen, G., Hetzler, B. G., Reyes-Spindola, J. F., and Miller, N. E. (2001) Radical SAM, a novel protein superfamily linking unresolved steps in familiar biosynthetic pathways with radical mechanisms: Functional characterization using new analysis and information visualization methods, *Nucleic Acids Res. 29*, 1097−1106.
19. Moss, M., and Frey, P. A. (1987) The role of S-adenosylmethionine in the lysine 2,3-aminomutase reaction, *J. Biol. Chem. 262*, 14859−14862.
20. Baraniak, J., Moss, M. L., and Frey, P. A. (1989) Lysine 2,3-aminomutase. Support for a mechanism of hydrogen transfer involving S-adenosylmethionine, *J. Biol. Chem. 264*, 1357−1360.
21. Ballinger, M. D., Frey, P. A., and Reed, G. H. (1992) Structure of a substrate radical intermediate in the reaction of lysine 2,3-aminomutase, *Biochemistry 31*, 10782−10789.
22. Wu, W., Lieder, K. W., Reed, G. H., and Frey, P. A. (1995) Observation of a second substrate radical intermediate in the reaction of lysine 2,3-aminomutase: A radical centered on the β-carbon of the alternative substrate, 4-thia-L-lysine, *Biochemistry 34*, 10532−10537.
23. Miller, J., Bandarian, V., Reed, G. H., and Frey, P. A. (2001) Inhibition of lysine 2,3-aminomutase by the alternative substrate 4-thialysine and characterization of the 4-thialysyl radical intermediate, *Arch. Biochem. Biophys. 387*, 281−288.
24. Magnusson, O. Th., Reed, G. H., and Frey, P. A. (2001) Characterization of an allylic analogue of the 5′-deoxyadenosyl radical: An intermediate in the reaction of lysine 2,3-aminomutase, *Biochemistry 40*, 7773−7782.
25. Lepore, B. W., Ruzicka, F. J., Frey, P. A., and Ringe, D. (2005) The X-ray crystal structure of lysine-2,3-aminomutase from *Clostridium subterminale*, *Proc. Natl. Acad. Sci. U.S.A. 102*, 13819−13824.
26. Lieder, K. W., Booker, S., Ruzicka, F. J., Beinert, H., Reed, G. H., and Frey, P. A. (1998) *S*-Adenosylmethionine-dependent reduction of lysine 2,3-aminomutase and observation of the catalytically functional iron−sulfur centers by electron paramagnetic resonance, *Biochemistry 37*, 2578−2585.
27. Chen, D., Ruzicka, F. J., and Frey, P. A. (2000) A novel lysine 2,3-aminomutase encoded by the *yodO* gene of *Bacillus subtilis*: Characterization and the observation of organic radical intermediates, *Biochem. J. 348*, 539−549.
28. Heinrikson, R. L., and Meredith, S. C. (1984) Amino acid analysis by reverse-phase high-performance liquid chromatography: Precolumn derivatization with phenylisothiocyanate, *Anal. Biochem. 136*, 65−74.
29. Chen, D., Frey, P. A., Lepore, B. W., Ringe, D., and Ruzicka, F. J. (2006) Identification of structural and catalytic activity of highly conserved amino acid residues in lysine 2,3-aminomutase, *Biochemistry 45*, 12647−12653.
30. Kennedy, M. C., Kent, T. A., Emptage, M., Merkle, H., Beinert, H., and Münck, E. (1984) Evidence for the formation of a linear [3Fe-4S] cluster in partially unfolded aconitase, *J. Biol. Chem. 259*, 14463−14471.
31. Beinert, H. (1983) Semi-micro methods for analysis of labile sulfide and of labile sulfide plus sulfane sulfur in unusually stable iron−sulfur proteins, *Anal. Biochem. 131*, 373−378.
32. Wada, H., and Snell, E. E. (1961) The enzymatic oxidation of pyridoxine and pyridoxamine phosphates, *J. Biol. Chem. 236*, 2089−2095.
33. Hewitson, K. S., Ollagnier-de Choudens, S., Sanakis, Y., Shaw, N. M., Baldwin, J. E., Münck, E., Roach, P. L., and Fontecave, M. (2002) The iron−sulfur center of biotin synthase: Site-directed mutants, *J. Biol. Inorg. Chem. 7*, 83−93.
34. Lees, N. J., Chen, W., Walsby, C., Frey, P. A., and Hoffmann, B. M. (2006) *J. Am. Chem. Soc. 128* (in press).
35. Wertz, J. E., and Bolton, J. R. (1986) *Electron Spin Resonance*, pp 164−174, Chapman and Hall, New York.
36. Fischer, H. (1973) in *Free Radicals* (Kochi, J. K., Ed.) Vol. II, pp 435−491, Wiley, New York.
37. Christenson, S. D., Wu, W., Spies, M. A., Shen, B., and Toney, M. D. (2003) Kinetic analysis of the 4-methylideneimidazole-5-one-containing tyrosine aminomutase in enediyne antitumor antibiotic C-1027 biosynthesis, *Biochemistry 42*, 12708−12718.
38. Gatto, G. J., Boyne, M. T., Kelleher, N. L., and Walsh, C. T. (2006) Biosynthesis of pipecolic acid by RapL, a lysine cyclodeaminase encoded in the rapamycin gene cluster, *J. Am. Chem. Soc. 128*, 3838−3847.

BI061328T